

Supporting Information

In-Situ Growth of Vertically Aligned FeCoOOH-Nanosheets/Nanoflowers on Fe, N co-doped 3D-Porous Carbon as Efficient Bifunctional Electrocatalysts for Rechargeable Zinc-O₂ Battery

Shumaila Ibraheem, Siguo Chen*, Jia Li, Qingmei Wang, and Zidong Wei*

The State Key Laboratory of Power Transmission Equipment & System Security and New Technology; Chongqing Key Laboratory of Chemical Process for Clean Energy and Resource Utilization, College of Chemistry and Chemical Engineering, Chongqing University, Chongqing 400044, China.

Email: csg810519@126.com, zdwei@cqu.edu.cn

1. Experimental Section

Preparation of 3D-FeNC: 8g KCl and 8g ZnCl₂ were dispersed in 40 mL deionized water at room temperature until well dissolved. Then the mixture was frozen immediately by directly inserting into liquid nitrogen for 5 minutes. The samples were then transfer to a freeze dryer at <0.05 mbar for 72 hours. 2.5g FeCl₃·6H₂O was dissolved into 1 mL ethanol and 1g *o*PD (*o*-phenylenediamine) was dissolved in 12 mL ethanol, respectively. Dark purplish-red precipitates were obtained by mixing of *o*PD, FeCl₃·6H₂O solutions. Then, the mixture was added drop wise into the ZnCl₂/KCl salt with continuous magnetic stirring for 60 minutes. Then, 2.5g NH₄S₂O₈ dissolved in 4mL HCl (1M) solution was added drop wise into above solution. After 1 h stirring and 24h quiet placing under room temperature, the reaction mixture was then poured into glass petri dishes and kept it to evaporate slowly under ambient conditions. The obtained dark-brown colored mixture was transferred into a muffle furnace; the temperature was raised to 800°C at a heating rate of 5°C min⁻¹ and maintained at 800°C for 2 hours under flowing N₂ environment. The obtained dark black powder was washed with 1 M HCl solution at 70°C for 8 h followed by centrifugation, washing and freeze-drying. The resulting products were second time carbonized at 900°C for 2 h with a heating rate of 5°C min⁻¹ under flowing N₂ environment and then collected final product.

Preparation of the FeCoOOH-NS ⊥ 3D-FeNC: Typically 0.1g 3D-FeNC was dissolved in a 100 mL solution which contains 75 mL ethylene glycol and 25 mL deionized water to obtain a homogenous solution by ultrasonically dispersion. After then 0.041375g FeCl₂·4H₂O, 0.0989g CoCl₂·6H₂O, (Fe/Co molar ratio was adjusted as 1:2) 0.151g AlCl₃·6H₂O and 0.5255g urea were subsequently added under strong magnetic stirring to produce salt solutions. Then the well

dissolved solution was heated at the refluxing temperature (about 90°C) under continuous magnetic stirring for 50 hours under flowing nitrogen. The resulting product was obtained by filtering, washing with ethanol and deionized water for several times. Finally the product was dried at room temperature and obtained as FeCoAl-LDH ⊥ 3D-FeNC. The high- concentrated alkaline solution treatment was applied to as obtained FeCoAl-LDH ⊥ 3D-FeNC to convert into FeCoOOH-NS ⊥ 3D-FeNC. Specifically 20.0 mg of FeCoAl-LDH ⊥ 3D-FeNC was added to 20.0 mL NaOH solution (6M) for 10 hours under continuous magnetic stirring. Finally the product was obtained by subsequent washing with anhydrous ethanol and deionized water for several times, and dried at room temperature. And catalyst was collected as FeCoOOH-NS ⊥ 3D-FeNC.

Preparation of the FeCoOOH-NF ⊥ 3D-FeNC: Nanosheets were successfully converted into nanoflowers by increasing the amount of Fe and Co content but interestingly the ratio of Fe and Co was adjusted same (1:2) as above. Typically 0.1g 3D-FeNC was dissolved in a 100 mL solution which contains 75 mL ethylene glycol and 25 mL deionized water to obtain a homogeneous solution by ultrasonically dispersion. After then 0.08275g FeCl₂.4H₂O, 0.1978g CoCl₂.6H₂O, 0.151g AlCl₃.6H₂O and 0.5255g urea were subsequently added under strong magnetic stirring to produce salt solutions. Then the well dissolved solution was heated at the refluxing temperature (about 90°C) under continuous magnetic stirring for 50 hours under flowing nitrogen. The resulting product was obtained by filtering, washing with ethanol and deionized water for several times. Finally the product was dried at room temperature and obtained as FeCoAl-LDH ⊥ 3D-FeNC. The high- concentrated alkaline solution treatment was applied to as obtained FeCoAl-LDH ⊥ 3D-FeNC to convert into FeCoOOH-NF ⊥ 3D-FeNC. Specifically 20.0 mg of FeCoAl-LDH ⊥ 3D-FeNC was added to 20.0 mL NaOH solution (6M)

for 10 hours under continuous magnetic stirring. Finally the product was obtained by subsequent washing with anhydrous ethanol and deionized water for several times, and dried at room temperature. And catalyst was collected as FeCoOOH-NF \perp 3D-FeNC.

Preparation of the FeCoOOH: For comparison the FeCoOOH was also prepared under same conditions and procedure without using the 3D-FeNC precursor.

2. Electrochemical measurements

Autolab electrochemical workstation was used to perform all the electrochemical tests for ORR/OER. The electrochemical measurements towards ORR/OER were recorded by three electrode method in which working electrode (glassy carbon rotating disk), a graphite rod as counter electrode and reference electrode (vs Ag/AgCl) were used in alkaline media (1.0 M KOH) under O₂ saturated and N₂ flooded. All potentials in this work are given relative to a reversible hydrogen electrode (RHE). For working electrode, homogenous catalyst ink was prepared by ultra-sonicating 2 mg of sample in 800 μ L ethanol and 20 μ L of Nafion (5% solution) under sonication for 30 minutes. Then, catalyst ink was dispersed on a glassy carbon surface (0.19625 cm²) followed by drying before the performance of tests. The loading of catalysts were \sim 0.25 mg cm⁻². Commercial 20 wt% platinum on Vulcan carbon black (Pt/C) and IrO₂ catalysts were used as the baseline catalysts. And working electrodes were prepared by total mass loadings of 40 μ g cm⁻² and 0.25 mg cm⁻² for the commercial 20 wt% Pt/C and IrO₂ catalyst respectively. The CV (Cyclic Voltammetry) and LSV (Linear Sweep Voltammetry) curves were recorded in 1.0 M KOH solution at 50 and 10 mVs⁻¹ of voltage sweeping rate, respectively for both ORR/OER. For ORR the accelerated durability test (ADT) was performed at room temperature in oxygen saturated 1.0 M KOH solution by applying cyclic potential sweeps

between 0.6 and 1.2 V at a sweep rate of 50 mV/s for 10,000 CV cycles. RDE measurements were performed by linear sweep voltammetry (LSV) at a scan rate of 10 mV s⁻¹ at various rotating speeds from 100 to 2500 rpm. For the ORR, the electron transfer numbers (n) were calculated with Koutechy-Levich equations.

$$\frac{1}{j} = \frac{1}{j_L} + \frac{1}{j_K} = \frac{1}{B\omega^{1/2}} + \frac{1}{j_K}$$

$$B = 0.62nFC_0(D_0)^{2/3}\nu^{-1/6}$$

$$j_K = nFkC_0$$

where j_K and j_L are the kinetic and diffusion-limiting current densities, j is the measured current density, respectively; ω is the angular velocity of the disk; F is the Faraday constant ($F = 96485$ C mol⁻¹); n represents the overall number of electrons transferred in oxygen reduction; D_0 is the diffusion coefficient of O₂ in 0.1 M KOH electrolyte (1.9×10^{-5} cm² s⁻¹); C_0 is the bulk concentration of O₂ (1.2×10^{-6} mol cm⁻³); ν is the kinematics viscosity for electrolyte, and k is the electron-transferred rate constant. Electrochemical impedance spectroscopy (EIS) measurements were recorded in O₂-saturated 1.0 M KOH at 0.80 V vs. RHE with 10 mV ac potential from 10 kHz to 0.01 Hz for ORR and at 0.30 V vs. RHE with 10 mV ac potential from 10 kHz to 0.01 Hz for OER. The loading was 0.25 mg cm⁻² for all materials. The electrode rotation speed was controlled at 1600 rpm

3. Zinc-O₂ batteries test

The zinc-O₂ battery was assembled using a self-made plastic cell. The gas diffusion layer (GDL) was made firstly by dispersing polytetrafluoroethylene (PTFE) emulsion (60 wt%, Saibo electrochemical) onto the back of carbon paper, and heated it at 340⁰C for 2 hours in muffle furnace. The oxygen electrode was prepared by transferring a certain volume of catalyst ink onto the carbon paper substrate with a catalyst loading of 0.25 mg cm⁻². A polished zinc plate (0.3 mm thickness) was used as anode. 6.0 M KOH was used as electrolyte for primary and rechargeable zinc-O₂ batteries to guarantee the reversible zinc electrochemical reactions at the Zn anode. The GDL has an effective area of 1 cm² and allows O₂ to reach the catalyst sites. Ni foam was used as current collector. All the zinc-O₂ batteries were tested under ambient atmosphere. The polarization curve measurements were performed by LSV (5 mV s⁻¹) at 25°C with Versa STAT 4 electrochemical working station. Both the current density and corresponding power density were normalized to the effective surface area of O₂ electrode. The specific capacity and energy density were calculated according the following equation:

$$\text{Specific Capacity} = \frac{\text{current} * \text{service hours}}{\text{weight of consumed zinc}}$$

$$\text{Energy Density} = \frac{\text{current} * \text{service hours} * \text{avarage discharge voltage}}{\text{weight of consumed zinc}}$$

The galvanostatic discharge-charge cycling (3 min discharge followed by 3 min charge) were carried out by LAND testing system.

4. Characterization

The Morphology of as made catalysts were characterized by FESEM, TEM and HRTEM. The field emission scanning electron microscope (FESEM) images were taken on a JSM-7800F (JEOL) scanning electron microscope recorded at an acceleration voltage of 8.0 kV. The transmission electron microscopy (TEM) was performed on a FEI Tecnai G2 F20 S-TWIN instrument operating at 120 kV. High-resolution transmission electron microscopy (HRTEM) was executed on a JEM-2100 instrument operating at 200 kV. High-angle annular dark-field scanning transmission electron microscope (HAADF-STEM)-energy-dispersive X-ray spectroscopy (EDS) was taken on Aztec X-Max 80 TEM operated at 200 kV with a spherical aberration corrector. The crystal structure was characterized by XRD. X-ray powder diffraction (XRD) data was recorded using a PANalytical X'pert diffractometer equipped with a PIXcel 1D detector (Cu K α radiation, $\lambda = 1.5406 \text{ \AA}$). The data were collected at voltage of 40 kV and current of 40 mA. The elemental contents were characterized by XPS analysis. X-ray Photoelectron Spectroscopy (XPS) was conducted on ESCALAB250Xi spectrometer equipped with a monochromatic Al X-ray source (Al KR, 1.4866 keV). The binding energies obtained in XPS spectral measurements were exactly corrected for samples charging by referencing C 1s to 284.5 eV. The specific surface area of all as made catalysts were measured using Brunauer-Emmett-Teller (BET) analysis and their adsorption and desorption isotherms, with experiments conducted at 77 K using a Kubo X1000 aperture and surface area analysis instrument.

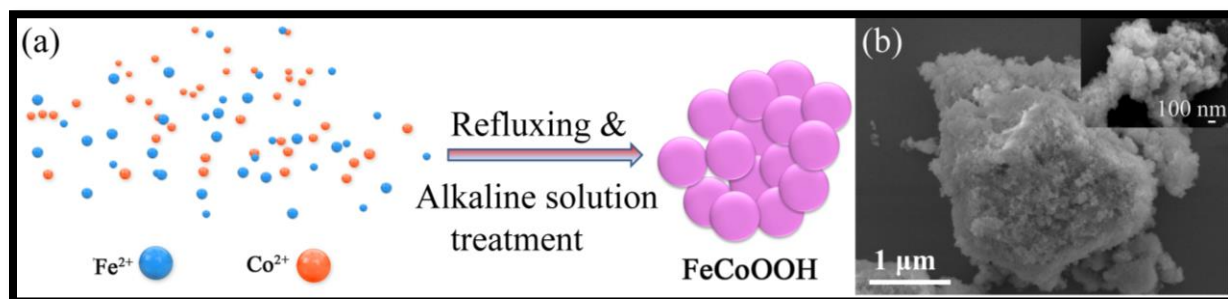


Fig. S1. (a) Schematic illustration of preparation of FeCoOOH. (b) FESEM images of FeCoOOH.

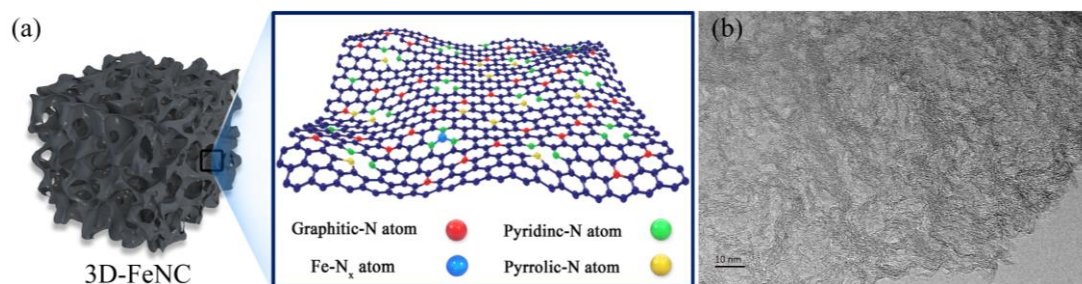


Fig. S2. (a) Schematic image of 3D-FeNC catalyst. (b) HRTEM image of 3D-FeNC catalyst.

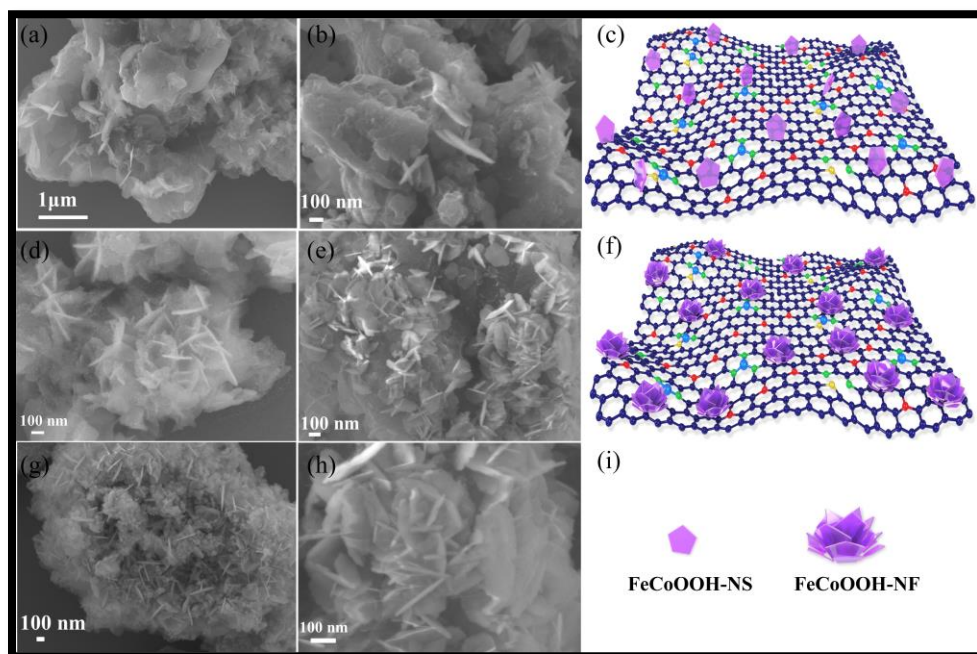


Fig. S3. (a-c) FESEM images of FeCoOOH-NS \perp 3D-FeNC catalyst and its schematic image. (d-h) FESEM images of FeCoOOH-NF \perp 3D-FeNC catalyst and its schematic image. (i) Schematic image of FeCoOOH nanosheet and nanoflower.

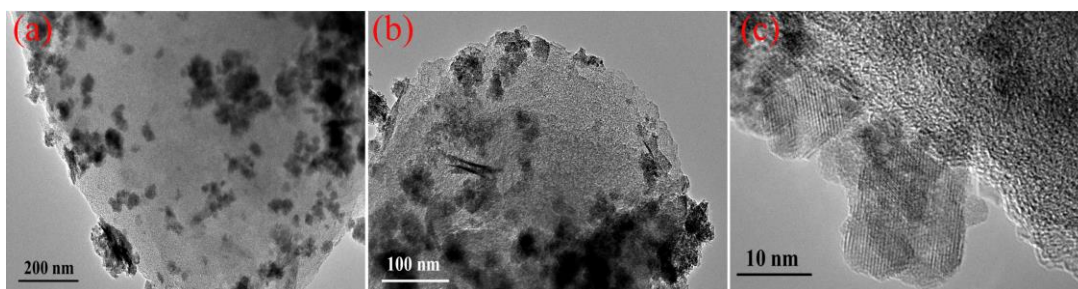


Fig. S4. (a,b) TEM images of FeCoOOH-NF \perp 3D-FeNC catalyst at different magnifications. (c) HRTEM image of FeCoOOH-NF \perp 3D-FeNC catalyst.

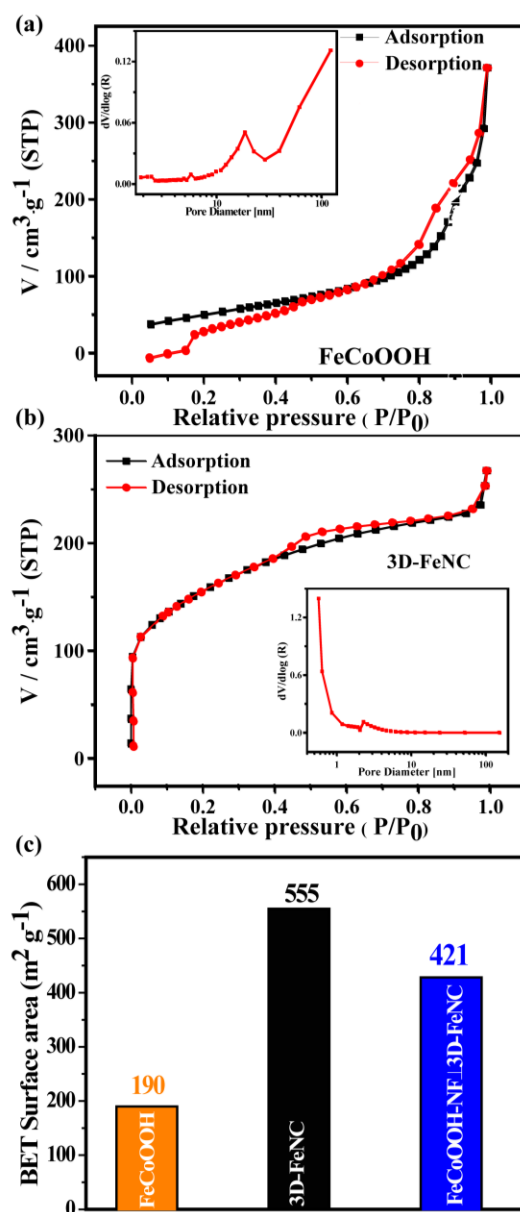


Fig. S5. (a, b) N_2 adsorption-desorption isotherms (inset: Barrett-Joyner-Halenda (BJH) pore-size distribution analysis curves). (c) BET surface areas of FeCoOOH, 3D-FeNC and FeCoOOH-NF \perp 3D-FeNC catalysts.

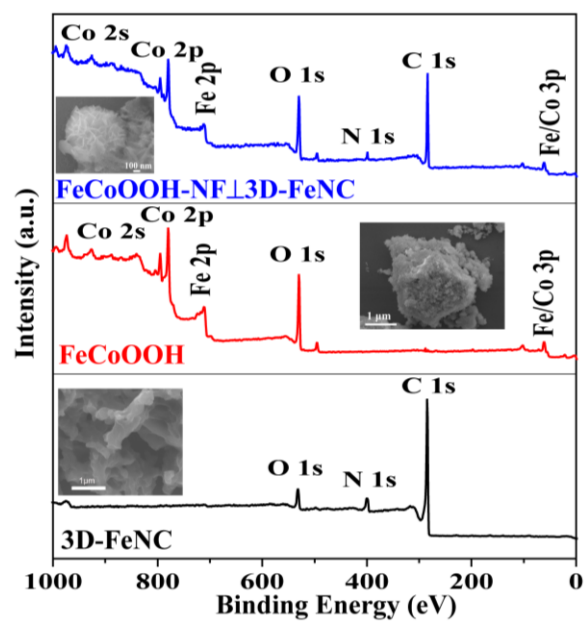


Fig. S6. XPS survey spectra of 3D-FeNC, FeCoOOH and FeCoOOH-NF \perp 3D-FeNC catalysts.

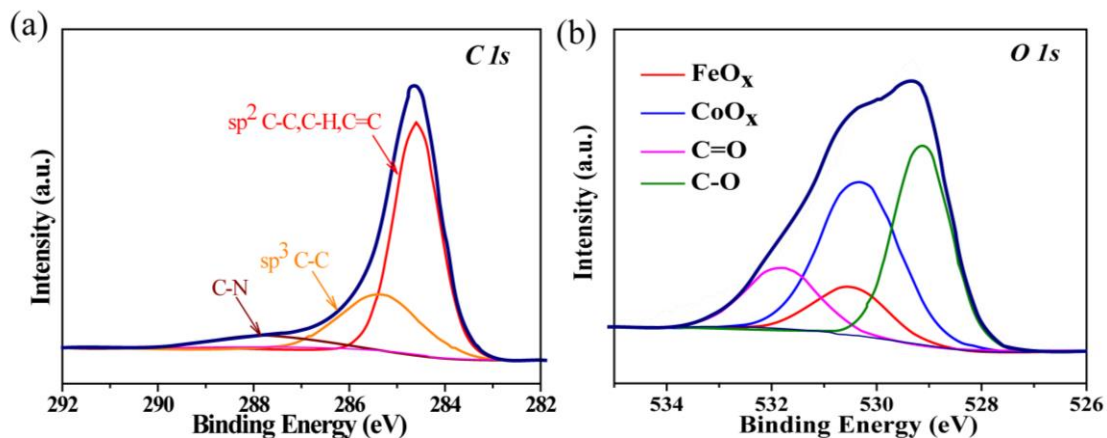


Fig. S7. High resolution C1s (a) and O1s (b) spectra of FeCoOOH-NF \perp 3D-FeNC catalyst.

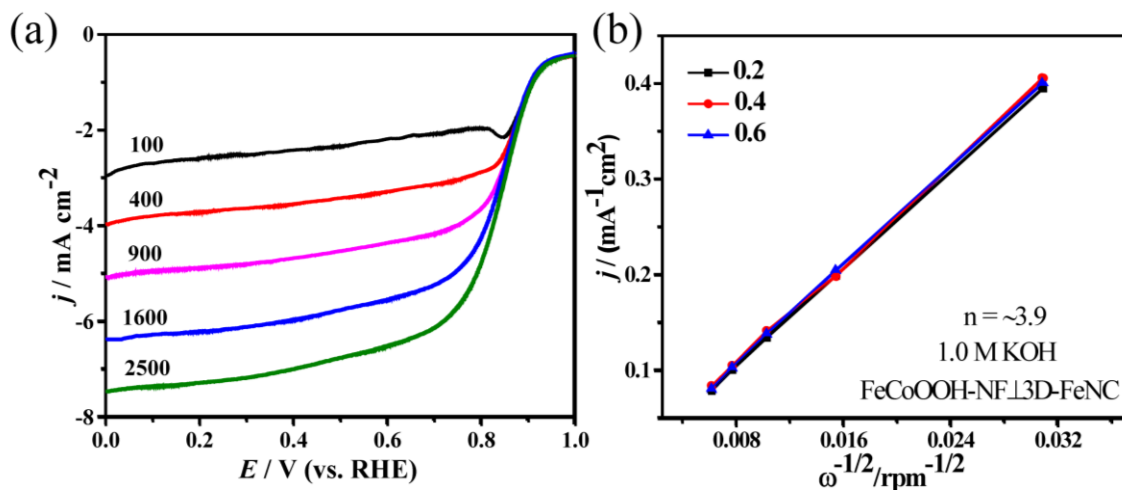


Fig. S8. (a) ORR polarization curves of FeCoOOH-NF \perp 3D-FeNC catalyst at different rotations.

(b) Corresponding Koutecky-Levich plot for electron transfer number (n).

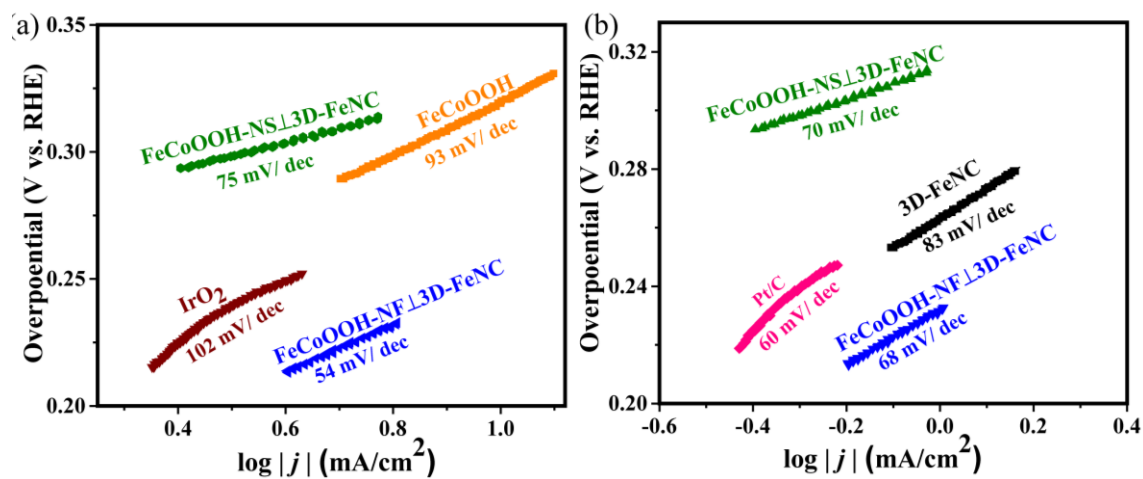


Fig. S9. (a) OER Tafel slopes. (b) ORR Tafel slopes.

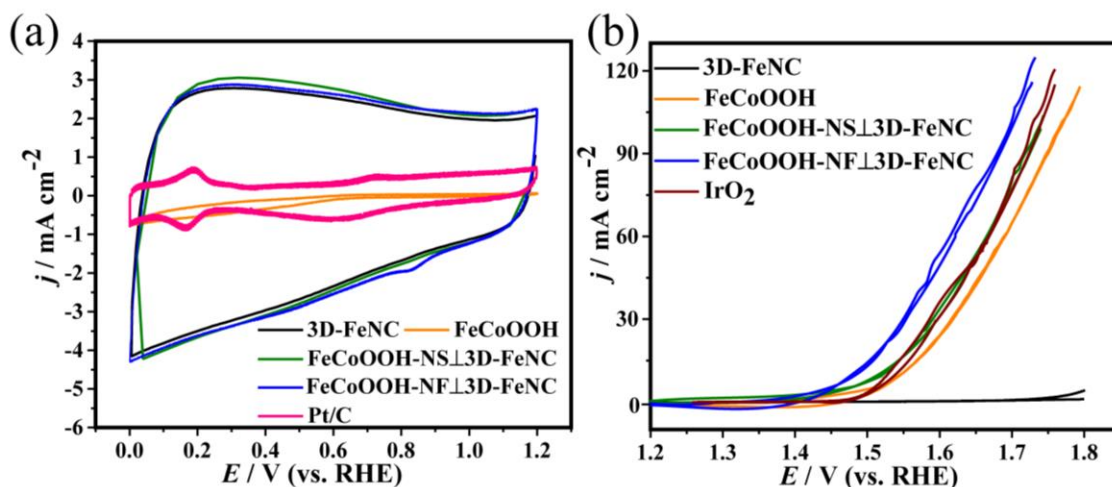


Fig. S10. (a) CV curves recorded in N_2 -saturated solution at room temperature with sweep rate of 50 mV s^{-1} . (b) CV curves recorded in N_2 -saturated at room temperature with sweep rate of 10 mV s^{-1} and rotation speed of 1600 rpm .

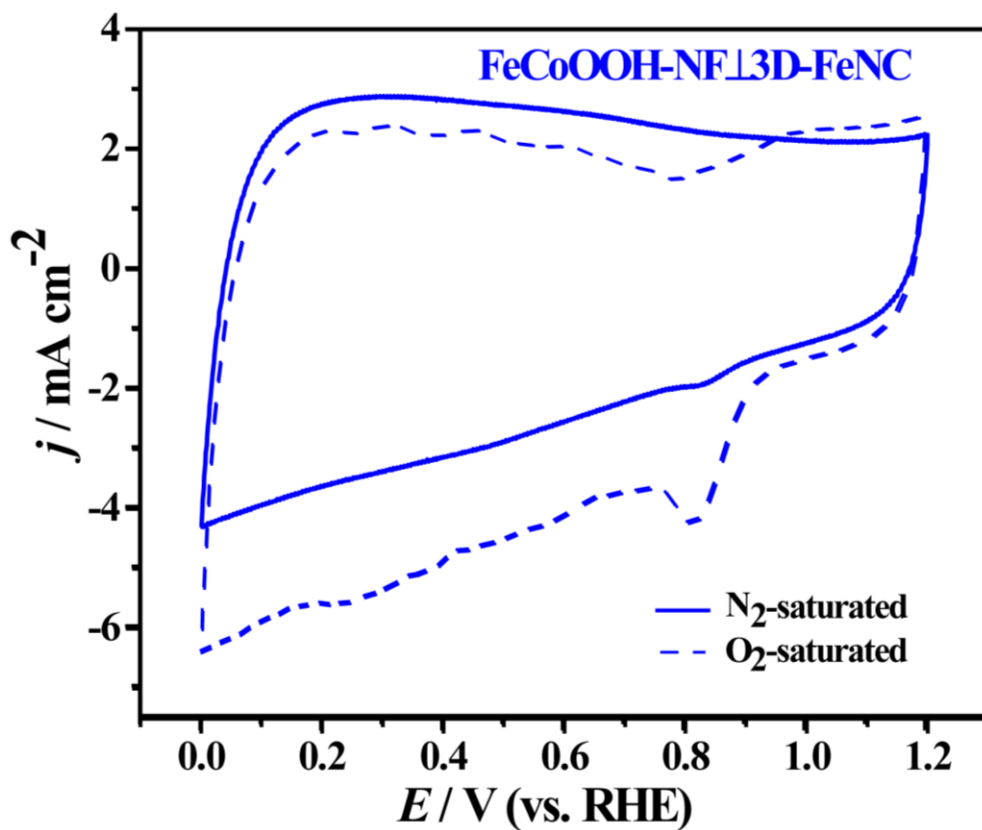


Fig. S11. CV curve recorded in N_2 -/ O_2 -saturated 1.0 M KOH solution at room temperature with a sweep rate of 50 mV s^{-1} .

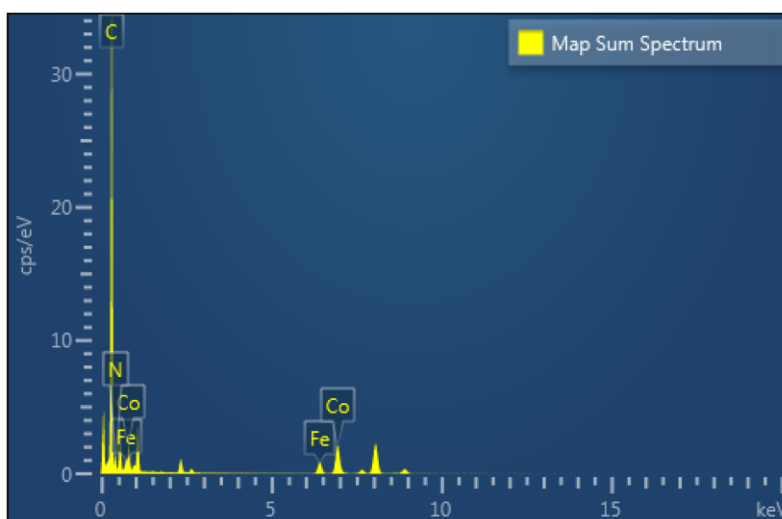


Fig. S12. EDX analysis of FeCoOOH-NF⊥3D-FeNC catalyst.

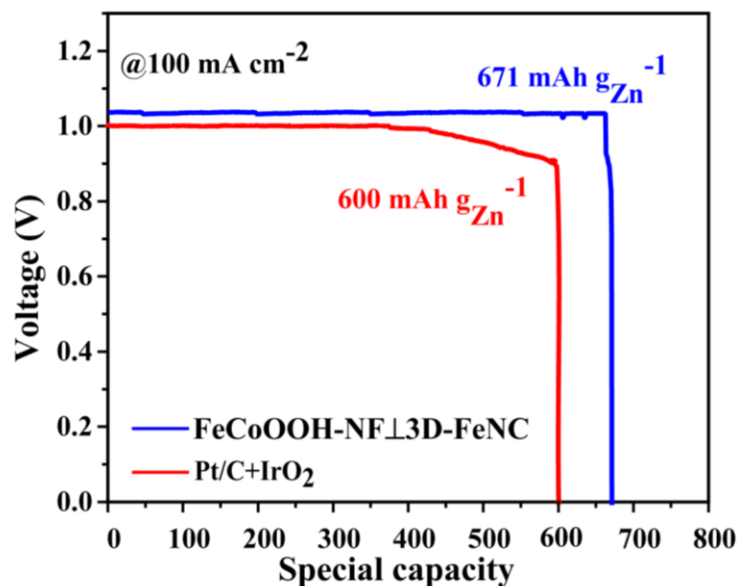


Fig. S13. Discharge curves of zinc-O₂ batteries assembled with FeCoOOH-NF⊥3D-FeNC and Pt/C+IrO₂ catalysts as cathode at 100 mA cm⁻² discharging rate.

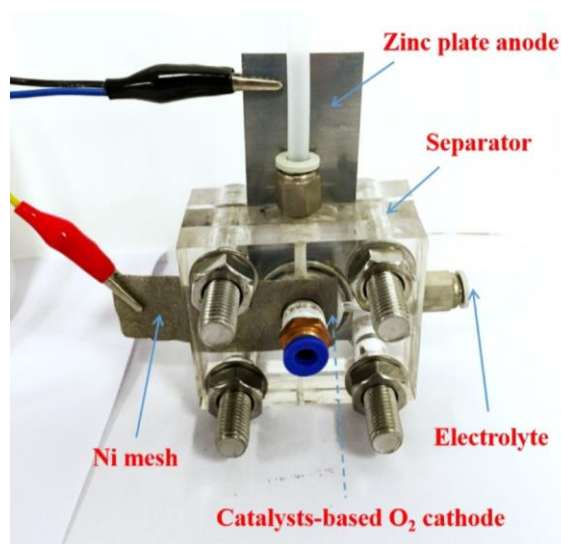


Fig. S14. Optical picture of zinc-O₂ battery. The pure 6.0 M KOH electrolyte was used as electrolyte for zinc-O₂ battery.

Table S1. Comparison of the elemental contents of 3D-FeNC, FeCoOOH, FeCoOOH-NS \perp 3D-FeNC and FeCoOOH-NF \perp 3D-FeNC catalysts obtained from XPS and ICP-MS measurements.

Sample	C(at.%)	N(at.%)	O(at.%)	Fe(at.%)	Co(at%)	ICP-MS Fe(wt%)	ICP-MS Co(wt%)
3D-FeNC	88.29	5.29	4.19	2.23	~	~	~
FeCoOOH	~	~	64.14	13.47	22.39	~	~
FeCoOOH-NS \perp 3D-FeNC	70.58	2.82	22.81	1.39	2.40	2.42	5.85
FeCoOOH-NF \perp 3D-FeNC	68.58	2.52	21.24	2.88	4.78	3.30	10.36

Table S2. Comparison of the Nitrogen configurations of 3D-FeNC and FeCoOOH-NF \perp 3D-FeNC catalysts obtained from XPS measurements.

Sample	Pyridinic-N/%	Fe-N _x /%	Pyrrolic-N/%	Quaternary-N/%	Oxidized-N/%
	~398.10eV	~399.20eV	~400.40eV	~401.90eV	~404.30eV
3D-FeNC	34.02	19.87	38.89	4.26	2.96
FeCoOOH-NF \perp 3D-FeNC	35.32	27.44	28.39	5.01	3.84

Table S3. Electrocatalytic performances evaluated for ORR and OER.

Sample	ORR			OER		
	$E_{1/2}$	Tafel	R_{ct}	$\eta@10$	Tafel	R_{ct}
	mV	mV/dec	Ω	mAc_m^{-2} (mV)	mV/dec	Ω
3D-FeNC	835	83	175	~	~	~
FeCoOOH	~	~	~	300	93	28.22
FeCoOOH-NS \perp 3D-FeNC	855	70	130	274	75	18.69
FeCoOOH-NF \perp 3D-FeNC	855	68	134	230	54	14.73
Pt/C (20%)	860	60	~	~	~	~
IrO ₂	~	~	~	311	102	~

Table S4. BET surface areas, pore volume of FeCoOOH, 3D-FeNC and FeCoOOH-NF \perp 3D-FeNC catalysts.

Sample	SBET (m ² g ⁻¹)	Pore volume (cm ³ g ⁻¹)
FeCoOOH	190.05	0.013
3D-FeNC	555.98	0.410
FeCoOOH-NF \perp 3D-FeNC	421.01	0.361

Table S5. Elemental content analysis of FeCoOOH-NF \perp 3D-FeNC by energy-dispersive X-ray analysis (EDX).

Element	Line Type	k Factor	Absorption Correction	Wt%	Wt% Sigma	Atomic %
C	K series	1.597	1.00	87.65	0.16	95.07
N	K series	2.028	1.00	3.06	0.15	2.85
Fe	K series	0.677	1.00	2.46	0.04	0.57
Co	K series	0.705	1.00	6.83	0.06	1.51
Total:				100.00		100.00

Table S6. Comparison of the ORR/OER activities of FeCoOOH-NF ⊥ 3D-FeNC catalyst with literature reprints electrocatalysts in alkaline electrolytes.

Sample	$E_{1/2}$ (V vs. RHE) (mV)	$\eta@10 \text{ mA cm}^{-2}$ (mV)	Loading ($\mu\text{g cm}^{-2}$)	Reference Electrode	Reference
FeCoOOH-NF ⊥ 3D-FeNC	855	230	250	RHE	This work
CoP-DC	790	321	283	RHE	S1
C-MOF-C2-900	815	421	200	RHE	S2
CMP@PNC	810	331	300	RHE	S3
S-Co ₉ -xFe _x S ₈ @rGO-10	840	290	500	RHE	S4
Fe/Co-CNTs-800	770	452	500	RHE	S5
AgCu-Mg	780	561	250	RHE	S6
0.1-Co-NHCs	810	~	217	RHE	S7
NiFeP@3D-FeNC	840	250	250	RHE	S8
Co/CoxSy@SNCF-800	740	313	400	RHE	S9
NC-Co ₃ O ₄ -90	870	358	250	RHE	S10

Table S7. Comparison of performance of rechargeable zinc-O₂ battery of FeCoOOH-NF ⊥ 3D-FeNC catalyst with other reported air electrocatalysts of zinc-air batteries.

Air catalysts	Open circuit voltage (V)	No. of Cycles	Reference
FeCoOOH-NF ⊥ 3D-FeNC	1.40	400	This work
cobalt (II/III) oxide/ nitrogen-doped CNT	1.31	20	S11
Fe ₃ Pt/Ni ₃ FeN	~	240	S12
nanoporous carbon nanofiber films	1.26	36	S13
NiFeP@3D-FeNC	1.40	144	S8
Ni _{0.75} Se	1.36	200	S14

References in Supporting information

- S1. Y. Lin, L. Yang, Y. Zhang, H. Jiang, Z. Xiao, C. Wu, G. Zhang, J. Jiang and L. Song, *Adv. Energy Mater.*, 2018, **8**, 1703623.
- S2. M. Zhang, Q. Dai, H. Zheng, M. Chen and L. Dai, *Adv. Mater.*, 2018, **30**, 1705431.
- S3. S. Yang, Q. He, C. Wang, H. Jiang, C. Wu, Y. Zhang, T. Zhou, Y. Zhou and L. Song, *J. Mater. Chem. A*, 2018, **6**, 11281-11287.
- S4. M. Zeng, Y. Liu, F. Zhao, K. Nie, N. Han, X. Wang, W. Huang, X. Song, J. Zhong and Y. Li, *Adv. Funct. Mater.*, 2016, **26**, 4397-4404.
- S5. Y.-M. Zhao, F.-F. Wang, P.-J. Wei, G.-Q. Yu, S.-C. Cui and J.-G. Liu, *ChemistrySelect*, 2018, **3**, 207-213.
- S6. X. Wu, F. Chen, N. Zhang, A. Qaseem and R. L. Johnston, *J. Mater. Chem. A*, 2016, **4**, 3527-3537.
- S7. S. Chen, J. Cheng, L. Ma, S. Zhou, X. Xu, C. Zhi, W. Zhang, L. Zhi and J. A. Zapien, *Nanoscale*, 2018, **10**, 10412-10419.
- S8. S. Ibraheem, S. Chen, J. Li, W. Li, X. Gao, Q. Wang and Z. Wei, *ACS. Appl. Mater. Interfaces*, 2019, **11**, 699-705.
- S9. S. Liu, X. Zhang, G. Wang, Y. Zhang and H. Zhang, *ACS. Appl. Mater. Interfaces*, 2017, **9**, 34269-34278.
- S10. C. Guan, A. Sumboja, H. Wu, W. Ren, X. Liu, H. Zhang, Z. Liu, C. Cheng, S. J. Pennycook and J. Wang, *Adv. Mater.*, 2017, **29**, 704117.

S11. M. Prabu, P. Ramakrishnan, P. Ganesan, A. Manthiram and S. Shanmugam, *Nano Energy*, 2015, **15**, 92-103.

S12. Z. Cui, G. Fu, Y. Li and J. B. Goodenough, *Angew. Chem. Int. Ed. Engl.*, 2017, **56**, 9901-9905.

S13. Q. Liu, Y. Wang, L. Dai and J. Yao, *Adv. Mater.*, 2016, **28**, 3000-3006.

S14. J. Wang, H. Wu, D. Gao, S. Miao, G. Wang and X. Bao, *Nano Energy*, 2015, **13**, 387-396